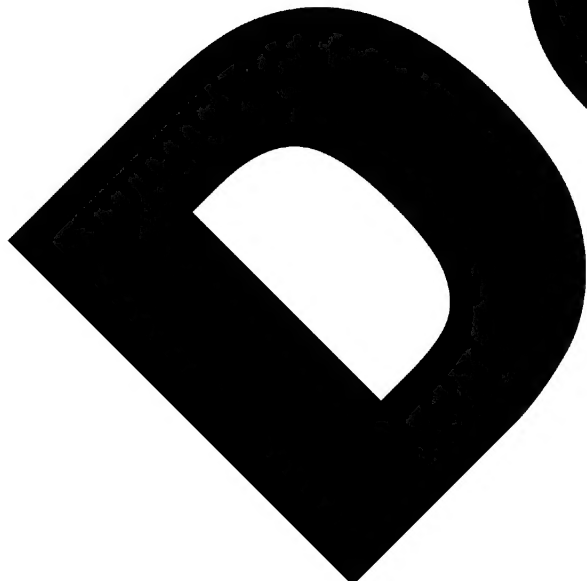


Approved For Release STAT
2009/08/26 :
CIA-RDP88-00904R000100110

 Approved For Release
2009/08/26 :
CIA-RDP88-00904R000100110



Third United Nations
International Conference
on the Peaceful Uses
of Atomic Energy

A/CONF.28/P/360
USSR

May 1964

Original: RUSSIAN

Confidential until official release during Conference

L.V. Maiorov, V.F. Turchin, M.S. Yudkevich.

THE CHEMICAL BINDING EFFECT ON NEUTRON THERMALIZATION.

INTRODUCTION

Computing slow neutron spectra in reactors one must take into account that slow neutron differential cross section are essentially influenced by the interatomic chemical bonds. This problem was solved in the past by means of simplified models. Now, owing to the development of slow neutron spectroscopy, it became possible to obtain from experiments necessary information on bound atom dynamics and, making use of previously developed theoretical methods,^X to compute adequately slow neutron differential cross-sections. It is well known, that a fine structure of differential cross-sections has only a minor influence on slow neutron spectra, so to calculate these it is quite sufficient to use an approximation which does not pretend to describe the fine structure but gives correct group constants with any reasonable choice of group widths. Such approximation, universally adopted nowadays, is the incoherent gaussian approximation, which assumes that neutron waves scattered by different atoms do not interfere and the space-time self-correlation function of an atom has a gaussian form.

In this report the methods of, and computer programs for, calculation of slow neutron group constants now used for reactor studies are described. The results of calculations for some moderators are presented and the influence of chemical binding on the integral parameters important for neutron thermalization, is studied. To analyze the influence of chemical bonds on neutron thermalization neutron spectra in infinite media are studied, as well as transient phenomena in space and time. The theoretical results are compared with the experimental data what may serve as a basis for the justification of one or another model of the atom dynamics.

^X Systematic treatment of the theory of slow neutron scattering together with the bibliography may be found in / 1/.

PROGRAM "UPRAS"

For multigroup differential cross section calculations a computer program UPRAS ("Universal Program for Cross Sections Calculations") was written in ALGOL-60 language and automatically translated into one of the machine languages.

On the first stage of its work this program calculates the symmetric scattering law $\tilde{S}(q, \epsilon)$, three modes of atomic motion being taken into account:

1. Acoustic vibrations with arbitrary spectrum. For small q the phonon expansion is used, for large q , the Egelstaff and Schofield formulae /2/ obtained by the steepest descent method may be used.

2. Optical vibrations with a zero width spectrum. (Optical vibrations with a spectrum of a finite width can be treated as a part of acoustic vibrations).

3. Diffusive motion with a half-width of the gaussian self-correlation function growing proportionally $|t|$ for large $|t|$. In the general case the scattering law is computed as a convolution of the scattering laws for specified modes with arbitrary weight coefficients. The scattering law calculated, the matrices $\tilde{G}(E_i \rightarrow E_j)$ and $\tilde{G}_1(E_i \rightarrow E_j)$ of zero and first angular moments of the double differential cross-sections are computed by integration. The matrices may be up to 50x50 order. Integral characteristics of the differential cross-section, such as \tilde{G}_S , $\tilde{\xi}$, $\cos \Theta$ etc., also are calculated.

The total cross section $\tilde{G}_t(E)$ and thermal neutron sources may be as well calculated by the program UPRAS to give full information for slow neutron spectra calculations.

PROGRAM "PRASSIV"

For the comparison of theoretical predictions with experimental results on the scattering of slow neutrons in solids and liquids a program PRASSIV ("Program for Calculation of Cross Sections by Time Integration") was written, which calculates in the incoherent gaussian approximation the double differential cross-sections of slow neutron scattering by a method, entirely different from the one described above.

In this program the symmetric scattering law is calculated by direct time integration of the well known Fourier-transformation

expression with a gaussian cut-off factor $\exp\{-\delta^2 t^2/2\}$ introduced into the integrand. The scattering law so calculated

$$\tilde{S}'(q, \varepsilon) = \frac{1}{2\pi} \int_{-\infty}^{\infty} \exp\{-q^2 \tilde{f}(t)\} \exp\{-\delta^2 t^2/2\} \cos \varepsilon t \, dt$$

is, due to a property of Fourier transformations, the convolution of the true scattering law $\tilde{S}(q, \varepsilon)$ with the gaussian of the width $\sim \delta$,

$$\tilde{S}'(q, \varepsilon) = \int_{-\infty}^{\infty} \tilde{S}(q, \varepsilon - \varepsilon') \frac{\exp\{-\varepsilon'^2/2\delta^2\}}{\sqrt{2\pi\delta^2}} \, d\varepsilon'$$

but this is just what one measures experimentally! The quantity δ determined by the resolution of the experimental device is specified in the program as a function of E_0 and E (for δ as a matter of fact strongly depends on E_0 and E). So the presence of the cut-off factor not only enables to calculate the scattering law by simple time integration, but also takes into account the experimental resolution when comparing the theory with experiment.

If there is no diffusive motion the function $\tilde{f}(t)$ is calculated through the normal frequency spectrum $g(\omega)$. The spectrum is arbitrary and the presence of optical vibrations does not complicate calculations. If the diffusive motion is present the function $\tilde{f}(t)$ is calculated by the interpolation formula proposed previously /1/, (at small t the diffusion motion does not essentially change the function in this model).

The program PRASSIV can compute double differential cross-sections $G(\varepsilon_0 \rightarrow \varepsilon, \theta)$ as well as differential cross-sections $G(\varepsilon_0 \rightarrow \varepsilon)$ and $G_1(\varepsilon_0 \rightarrow \varepsilon)$ and their integral characteristics. It can be used for multigroup matrices calculations if only δ is taken not larger than the group width.

Differential cross-sections.

We shall briefly characterize the problems arising in the calculation of differential cross-sections for some important moderators and present some results of calculations.

Water The frequency spectrum of the vibrations of a hydrogen atom in a water molecule can be represented as a sum of two terms. The first ("acoustic") one describes acoustic vibrations and hindered rotations of the molecule and extends up to approximately 0.13 ev. The second ("optical") term describes the vibrations of the hydrogen atom in the molecule, characteristic frequencies being $\sim 0,2$ ev

and $\sim 0,48$ ev. Krieger and Nelkin /3/ found the weight of the "acoustic" term $A_a = 0.48$. This value was used in our calculations. The form of the "acoustic" spectrum was determined by Larsson /4/ from the scattering of cold neutrons and by Egelstaff /5/ and Mostovoy /6/ from double neutron spectrometer measurements by means of the Egelstaff extrapolation technics /7/.

The differential cross-section $\bar{G}(E_0 \rightarrow E)$ with initial energy $E_0 = 0,102$ ev was calculated by the program PRASSIV, two frequency spectra being used: those by Larsson and by Egelstaff. The results were compared with the experimental results of Mostovoy (see Fig.1). One can see that the cross-section calculated with the Egelstaff frequency spectrum agrees well with experiment, so this spectrum was adopted for differential cross-section calculations to be used for neutron thermalization studies in water.

The integral characteristics of differential cross-sections are less sensitive to the form of the "acoustic" spectrum than differential cross-sections themselves, which can be seen from figures 2 and 3 where the mean logarithmic energy loss ξ and the average cosine of the scattering angle $\overline{\cos \Theta}$ are shown. Theoretical curves for both spectra agree well with experiment.

Graphite Various theoretical approaches give different frequency spectra of graphite lattice vibrations. The experimental determination of frequency spectrum from neutron scattering data by the Egelstaff extrapolation method is not very reliable because of strong coherence of the scattering. But for reactor studies a model which gives, accurate enough, the integral characteristics of scattering cross-sections is quite satisfactory. Such a model was proposed by Egelstaff /8/. Using this model, some investigations were carried out of neutron thermalization in space and time, which will be described below. Besides, the differential scattering cross-section was calculated with a frequency spectrum obtained by Baldock /9/. The integral characteristics of the differential cross-sections calculated by these two models were compared. The distinctions are not very large. The mean energy loss is shown in Fig.4 as an example.

Beryllium. The high symmetry of beryllium crystal lattice affords to use the Debye model with the Debye temperature $\Theta = 1000^{\circ}\text{K}$ found from

heat capacity measurements. In Fig.5 the differential cross-section $\sigma(E_0 \rightarrow E)$ for the Debye crystal with the atom mass 9 is shown in order to demonstrate the work of the program PPASSIV when energies are large. The temperature T was taken equal to the Debye temperature Θ . The energy E is measured in initial energy E_0 units.

For $E_0 = 60\Theta$ the differential cross-section approaches to the plateau containing curve specific for the scattering on a free atom.

Zirconium hydride. The frequency spectrum of vibrations of a hydrogen atom in zirconium hydride has an optical part with the average energy about 0,13 ev and the half-width about 0,025 ev and an acoustic part with the Debye temperature about 0.02 ev /10/, [23].

The weights of these are approximately in the ratio of the Zr mass to the H mass. This information is sufficient to construct an approximate frequency spectrum. By means of the program PRASSIV one can use experimental double differential cross-section (at one angle and initial energy only) to correct a frequency spectrum so as to fit the experimental points. The energy distribution of neutrons with initial energy 0,020 ev scattered at the angle 80° which was obtained by V.A. Parfenov et al. on the double neutron spectrometer using pulsed fast reactor in Dubna /11/, is shown in Fig. 6.

The theoretical curve was computed by the program PRASSIV with the corrected frequency spectrum.

Lithium hydride. According to /23/ the frequency spectrum of vibrations of a hydrogen atom in lithium hydride was taken as consisting of two optical lines: 0,10 ev and 0,13 ev with weight ratio 2 : 1 and an acoustic part with the Debye temperature $\Theta = 250^\circ\text{K}$ and the weight $M_H / (M_H + M_{Li}) = 0.125$. In Fig.7 the total scattering cross-section in lithium hydride computed by the program "UPRAS" is shown in comparison with the experimental points of Doilnitsyn et al. /12/.

Spectra in infinite media.

The chemical bond effect on the neutron thermalization can be appreciated by the investigation of its influence on various integral characteristics of neutron spectra. In particular, one of the most important thermalization characteristics of a moderator is the neutron gas temperature in an infinite media with not very large $1/\nu$

absorption, when the energy distribution of thermal neutrons can be treated as a maxwellian one.

For three hydrogenous moderators: water, zirconium hydride and lithium hydride, the neutron spectra in an infinite medium at $T=300^{\circ}\text{K}$ poisoned by the $1/\nu$ -absorber were computed for several values of absorption cross-section varying up to 10 barn per hydrogen atom. The spectra in water and lithium hydride are nearly maxwellian with a certain effective temperature T_n . The spectra in zirconium hydride (see Fig.8) are essentially non-maxwellian in the vicinity of vibrational quantum energy, but still it is possible to determine the effective temperature T_n from the lower energy region.

In order to represent in a convenient way the dependence of effective neutron temperature T_n on the absorption cross-section, we small make use of the formula

$$T_n/T = 1 + \alpha (\bar{\sigma}_a/\bar{\sigma}_s)$$

where $\bar{\sigma}_a$ is the absorption cross-section per hydrogen atom at the energy $E = T$, and $\bar{\sigma}_s = 20,4 \text{ b.}$ is total scattering cross-section on the free hydrogen atom. The coefficient α can be understood as an effective mass of moderator: $\alpha = m_{e\delta}$, for in the moderation of neutrons by an ideal monatomic gas is approximately equal to the mass of the atom /13/. The dependence of $m_{e\delta}$ on $\bar{\sigma}_a$ for the three moderators is shown in Fig.9. The strong dependence of $m_{e\delta}$ on $\bar{\sigma}_a$ for zirconium hydride follows from the fact that the pattern of the slowing down process in zirconium hydride is quite different from that in a heavy gaseous moderator. On the contrary, the nearly constant and close to unity value of $m_{e\delta}$ for water testifies that as it was noticed before by its' slowing down properties water is close to free hydrogen atoms. For water and lithium hydride the calculated results agree well with the experimental data /12/,/14/.

The rethermalization length.

In dealing with reactors with large temperature gradients it is important to know at what distance from the temperature discontinuity surface a neutron spectrum with local temperature is settled .

This distance is characterized by so called thermalization or rethermalization length l_{th} , which for the plane geometry is defined through the relation

$$T_n(x) - T_n(\infty) = \text{const} \exp\{-x/l_{th}\}$$

where $T_n(x)$ is the neutron gas temperature at the distance x from the temperature discontinuity plane. The rethermalization length is essentially dependent on the chemical bonds between moderator atoms and is one of the important characteristics to judge on the chemical bond effect. As an example we present the results of a calculation of neutron space-energy distribution in a graphite cylinder consisting of two zones with different temperatures. The inner zone with a radius of 40 cm has a temperature of 300°K . The outer zone with a radius 80cm has a temperature of 450°K . In Fig.10 the neutron gas temperature T_n against the distance from the cylinder axis is shown, calculated with the ideal gas model ($M=2$) differential cross-sections and with cross-sections computed by the program UPRAS with the Egelstaff vibration frequency spectrum [8]. For free graphite atoms $L_{th}=4.2$ cm, for bound atoms $L_{th}=6.9$ cm. As the rethermalization length for ideal monatomic gas increases with M as \sqrt{M} we may say that the effective mass of a bound graphite atom is about 32. The rethermalization calculations were carried out by the program T-2 (P-1 approximation, 40 energy groups).

Pulsed neutron thermalization.

A great deal of information on slow neutron scattering by bound atoms is contained in pulsed neutron source experiments. So the comparison with these experiments is a good check for a theory. For this purpose a program " TEDI" (Thermalization and Diffusion) was written in ALGOL-60 language, which calculates in the P-1 approximation the time dependent energy distributions of neutrons in a finite moderator block. A system of two differential equations for neutron density $N(E,t)$ and flow $J(E,t)$ is solved by the Runge-Kutta method for a space component with given B^2 . The maximum number of energy groups is 30.

The time dependence of the average neutron velocity in water is shown in Fig.11. In about 12 msec after the pulse the effective neutron temperature T_n begins to approach the media temperature T exponentially: $T_n - T = \text{const} \exp\{-t/t_{th}\}$, with a thermalization time $t_{th} = 4.6$ mc sec.

For graphite the exponential dependence settles at about 800 mc sec, the thermalization time being equal to 315 mc sec (at the density of 1.6 gr/cm³).

A special attention was paid to the investigation of asymptotic neutron spectra at large time when $N(E, t) = n(E)e^{-\alpha t}$, $J(E, t) = I(E)e^{-\alpha t}$.

The dependence of the decay constant α on B^2 was measured for various moderators by many authors. From these measurements the diffusion coefficient D_0 and diffusion cooling C were determined. It is well known that the equation for the asymptotic energy distribution of neutrons in the stationary diffusion process differs from that in the pulsed source case only by the sign of buckling B^2 .

Measuring diffusion length as a function of absorption cross-section it is possible to find out α as a function of B^2 in the negative B^2 region. Thus the asymptotic spectra and the constant α were calculated by the program TEDI both for positive and negative values of B^2 .

The calculated asymptotic density and flow neutron spectra are shown in Fig.12 for water and Fig.13 for graphite at different values of B^2 . For both moderators the density and flow spectra differ appreciably. The effect of diffusion cooling for $B^2 > 0$ and diffusion heating for $B^2 < 0$ is clearly seen. It may be worthwhile to note at the energies larger than $T_n(E)$ and $I(E)$ are Maxwellian with some effective temperature T_n depending on B^2 .

In Fig.14 the function (B^2) for water at the temperature of 295°K is shown. The differential cross-sections were calculated by the program UPRAS with the frequency spectrum of Egelstaff [5].

The experimental points are taken from [15] and [16] (pulsed source measurements) and [17] (poisoning experiments). The agreement of the theory with poisoning experiments (negative B^2) is very good. In the positive B^2 region the theory agrees well with the measurements by Lopez and Beyster [15] and somewhat diverges from those by Antonov [16] and Küchle [18] (Küchle's data are not shown in the figure).

We must note that the experiments of Lopez and Beyster were carried out

in a rectangular geometry while the experiments of Antonov and Kuchle - in a cylindrical geometry in which case the determination of B^2 is less sound. The calculated values of the parameters are:

$$D_0 = 3.66 \cdot 10^4 \text{ cm}^2/\text{sec}, C = 3.08 \cdot 10^3 \text{ cm}^3/\text{sec}$$

On the whole one may conclude that the use of the Egelstaff frequency spectrum for water leads to a good description of neutron thermalization and diffusion.

The function $\alpha(B^2)$ for graphite at the temperature of 295°K is shown in Fig. 15. The differential cross-sections were calculated by the program UPRAS with the model frequency spectrum of Egelstaff /8/. Since there is no data on the poisoning method, the calculations were carried out only for $B^2 = 0$. The experimental points are from /19/ and /20/. For large dimensions of moderator blocks the theory agrees well with the experiments, which implies that the calculated diffusion coefficient $D_0 = 2.12 \cdot 10^5 \text{ cm}^2/\text{sec}$

is very close to the experimental value. For smaller dimensions the theory gives larger D_0 , which implies that the theoretical value of the diffusion cooling constant $C = 1.95 \cdot 10^6 \text{ cm}^3/\text{sec}$ is smaller than the experimental value.

CONCLUSION

Owing to the intensive work on the neutron thermalization problem carried out in various countries the experimental and theoretical methods are available at present, which make possible to obtain the differential cross-sections of slow neutron scattering on bound atoms and check them by comparison with experimental data on neutron spectra. Added to the up-to-date computational methods (see for instance /21/, see also /22/) this makes possible for any system of interest to calculate the space-energy distribution of slow neutrons and effects resulting from its variation.

References.

1. V.F. Turchin, *Medlennye nejtrony* (Slow neutrons) Gosatomizdat, 1963.
2. G. Vineyard. *Phys. Rev.* 110, 999 (1958). P.A. Egelstaff, P. Schofield. *Nucl. Sci. Eng.*, 12, 260, (1962).
3. T.J. Krieger, M.S. Nelkin, *Phys. Rev.* 106, 290 (1957).
4. K.E. Larsson, U.J. Dahlborg, *Nucl. Energy* 16, 81 (1962).
5. P.A. Egelstaff et al. "Inelastic scattering of neutrons in solids

and liquids", Vienna 1963, v. I, p. 343.

6. V. I. Mostovoy. This conference report.

7. P. A. Egelstaff, Nucl. Sci. Eng. 12, 250 (1962).

8. Y. D. Macdougall. Brookhaven Conference on Neutron Thermalization vol. I, p. 121 (1962).

9. G. R. Baldock, Phil. Mag. I, 789 (1956).

10. A. McReynolds et al. 2-nd Geneva Conference, Report N1540.

11. I. I. Bondarenko et al. Inelastic scattering of neutrons in solids and Liquids. vol I. p. 127. Vienna 1963.

12. Ye. Ya. Doilnitsyn et al. This conference report.

13. R. R. Coveyou et al., J. Nucl. Energy, 2, 153 (1956).

14. Ye. Ya. Doilnitsyn and A. G. Novikov, Atomnaja Energija 13, 491 (1962).

15. W. M. Lopez, I. R. Beyster, Nucl. Sci. and Eng. 12, 190 (1962).

16. A. V. Antonov. Issledovaniya po jadernoj fizike (Nuclear physics investigations) vol XIV, p. 147 (1962).

17. E. Starr, I. Koppel, Brookhaven Conference on Neutron Thermalization, 1962.

18. M. Klichle, Nucleonik 2, 131 (1960).

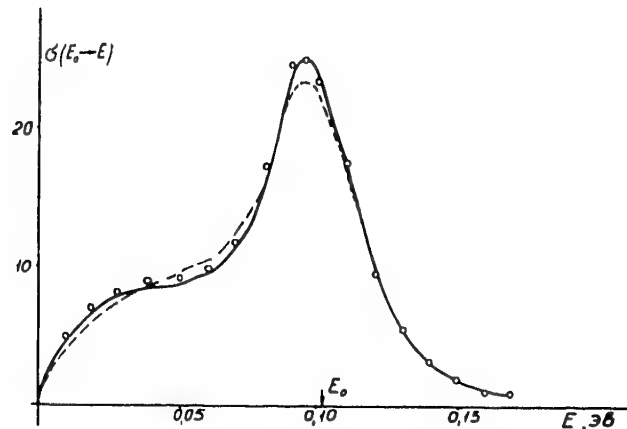
19. E. Starr and G. A. Price, Brookhaven Conference on Neutron Thermalization 1962.

20. D. Brune, Jirlow, J. of Nuclear Energy, Part A.B. 17, 349 (1963).

21. G. I. Marchuk. Metody rascheta jadernykh reaktorov (Methods of nuclear reactor calculations), Gosatomizdat 1961.

22. G. I. Marchuk et al. This conference report.

23. Inelastic scattering of neutrons in solids and liquids". Vienna 1961.



Puc. 1.

Fig. I. The differential scattering cross-section in water at $E_0 = 0,102\text{ev}$. The solid curve is calculated with the Egelstaff frequency spectrum/5/, the dotted one with the Larsson spectrum/4/. The experimental points are from Mostovoy et al /6/.

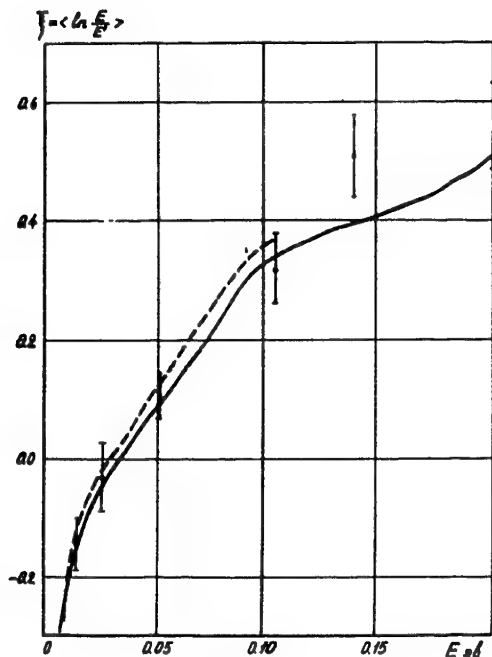


Fig. 2. The mean logarithmic energy loss ξ of neutrons in water. The solid curve is calculated with the Egelstaff spectrum, the dashed one with that of Larsson. The experimental points are from /6/.

Puc. 2.

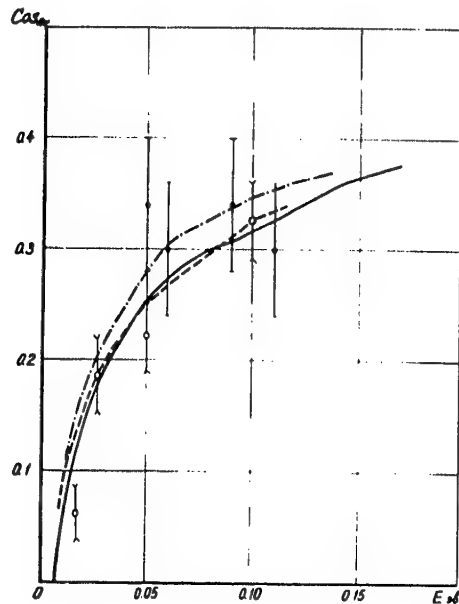


Fig. 3. The average cosine of the scattering angle of neutrons in water. The solid curve is calculated with the Egelstaff spectrum. The dashed curve with Larsson's, the dot-dashed curve the Nelkin model. The experimental points are from 6 (empty circles) and 8 (filled circles).

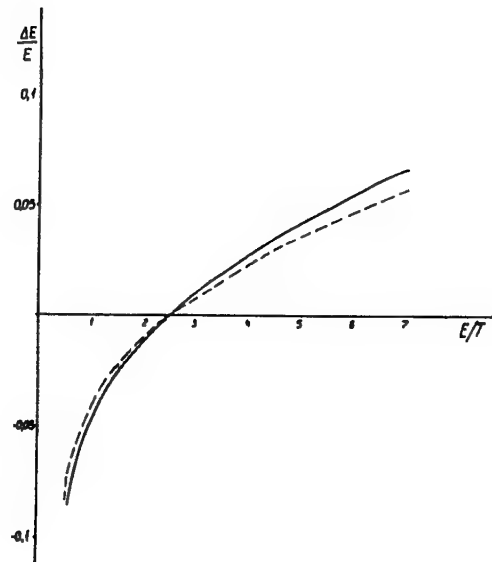


Fig. 4. The mean energy loss in graphite with the frequency spectrum of Egelstaff 8 (solid curve) and Baldock 9 (dashed curve).

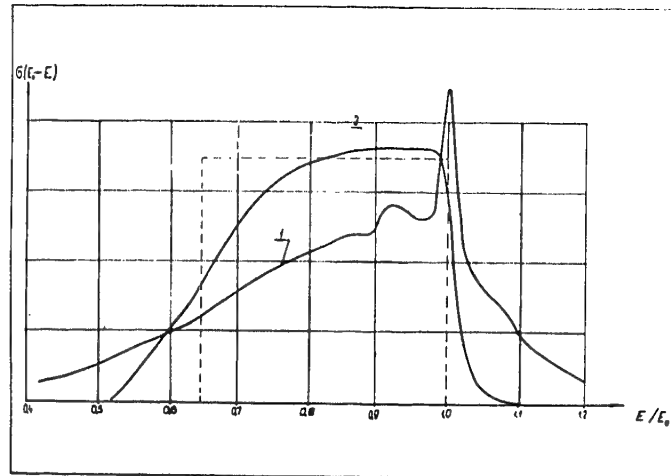


Fig. 5. The differential cross-section $G(E_i \rightarrow E)$ of neutron scattering on a Debye crystal with $M=9$.
 1.- initial energy $E = 100 \text{ eV}$. 2 - $E_i = 600 \text{ eV}$.

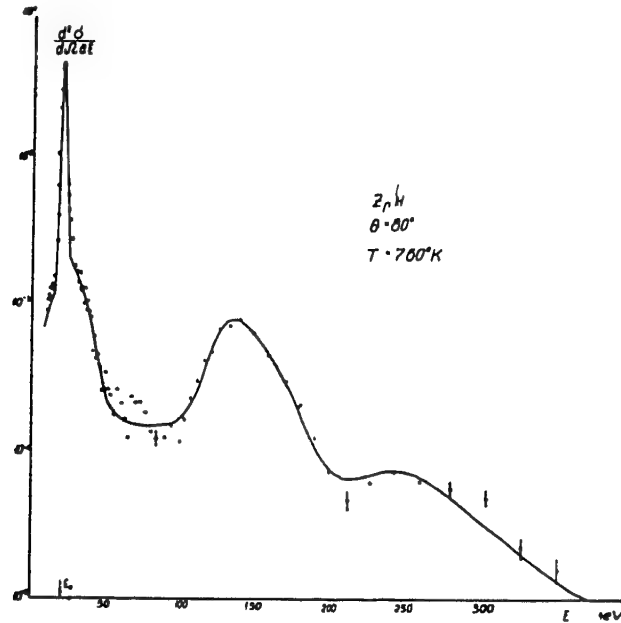


Fig. 6. The energy distribution of 20 mev neutrons scattered at the angle of 80° on the zirconium hydride sample at the temperature of 760°K . The theoretical curve is calculated by the program PRASSIV taking into account the experimental resolution.

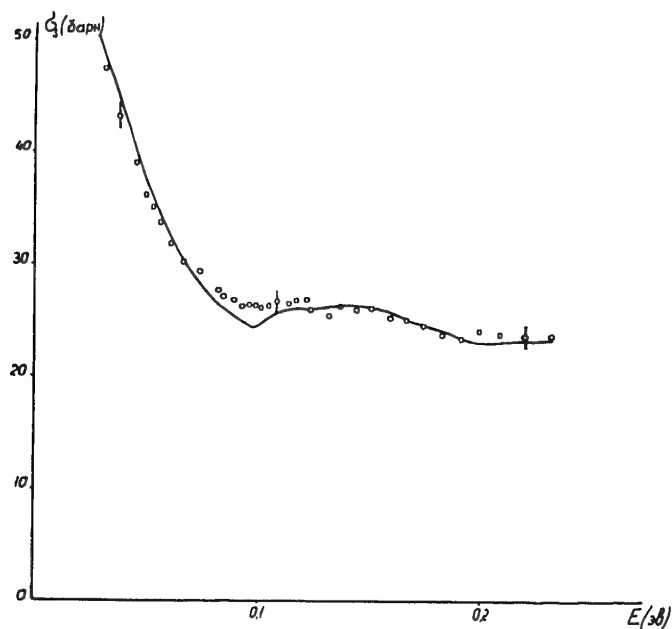


Fig. 7. The total scattering cross-section on a hydrogen atom in lithium hydride.

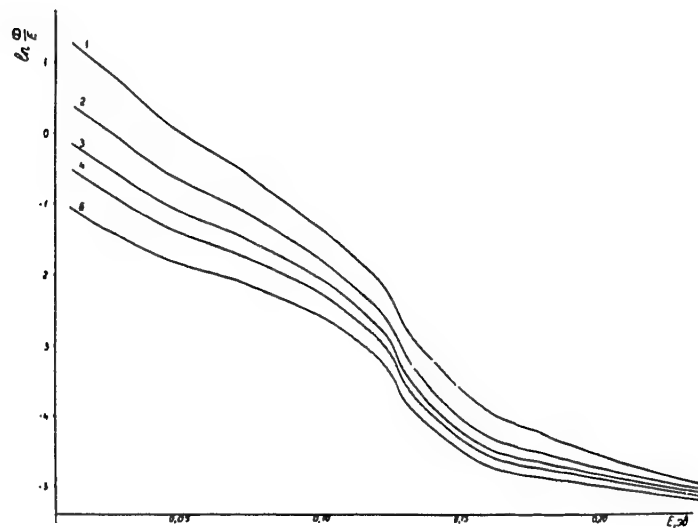


Fig. 8. The netron spectra in an infinite medium of zirconium hydride poisoned by $\frac{1}{2}$ -absorber at the room temperature. The figures at the curves denote the absorption cross-section at $E = 0.025$ ev in barns per a hydrogen atom.

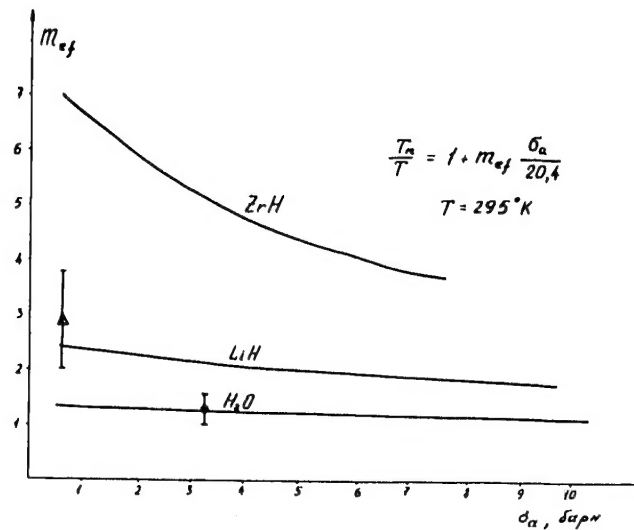


Fig. 9. The effective mass of three hydrogenous moderators, \circ - the experimental value for water I4
 Δ - that for lithium hydride I2.

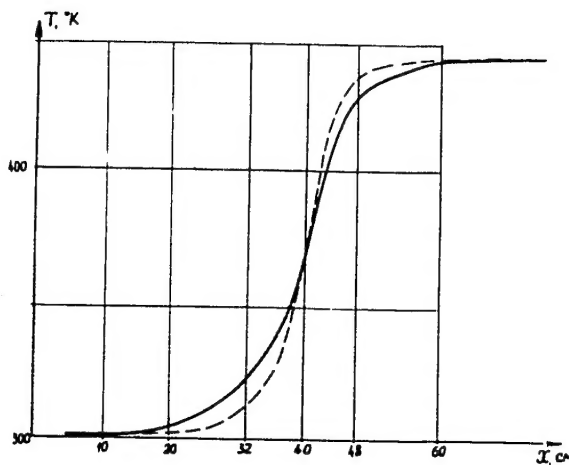


Fig. 10. The neutron gas temperature in a graphite cylinder consisting of two zones with the temperatures of $300^{\circ} K$ AND $450^{\circ} K$. The solid curve is calculated with the bound atom differential cross-section, the dashed curve by gas model.

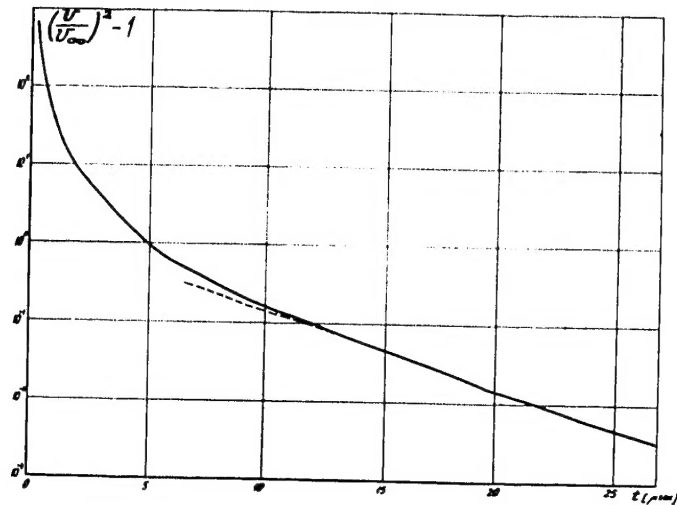


Fig.II. The average neutron velocity in water as a function of time

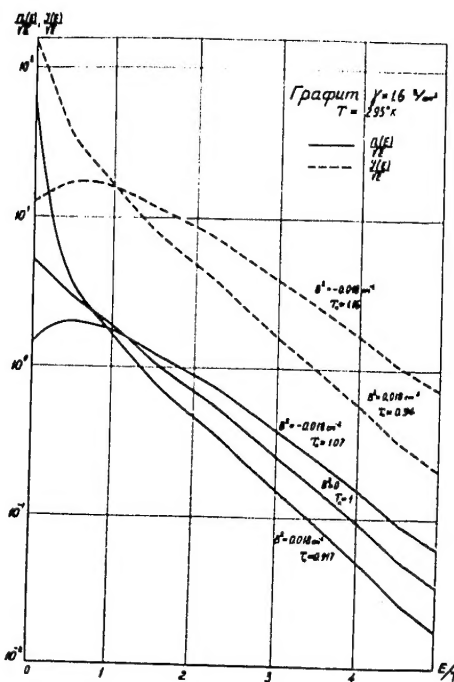


Fig.I3. The asymptotic neutron density and flow distribution in graphite

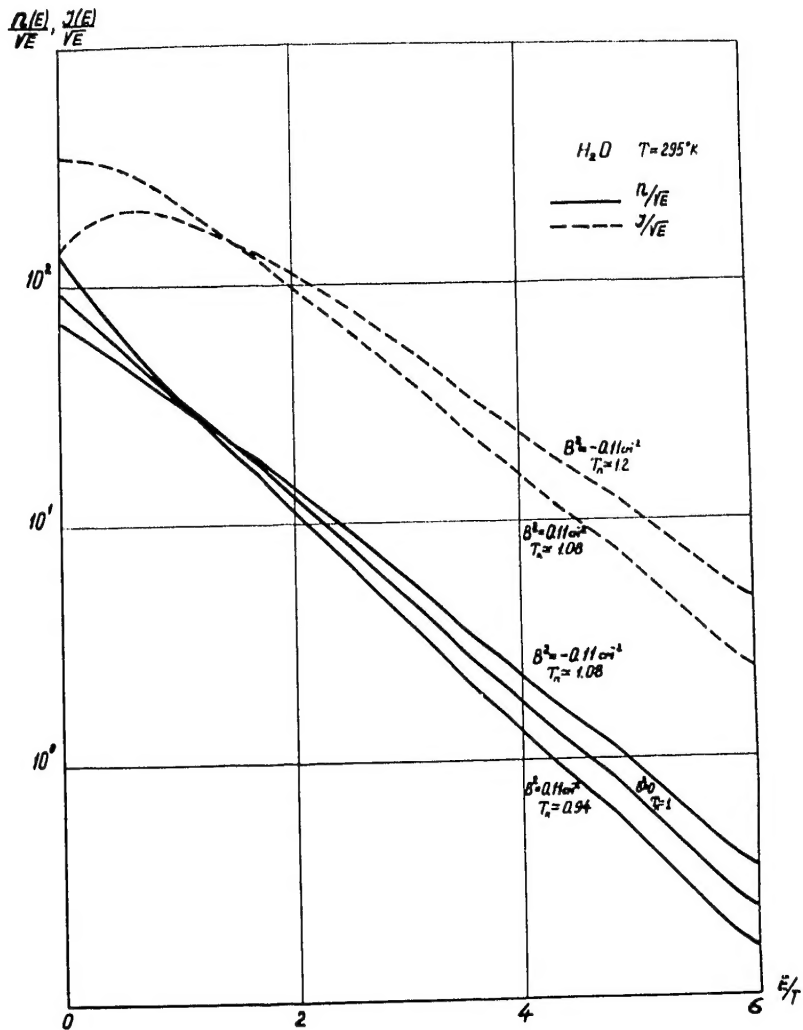


Fig. I2. The asymptotic neutron density and flow distribution in water

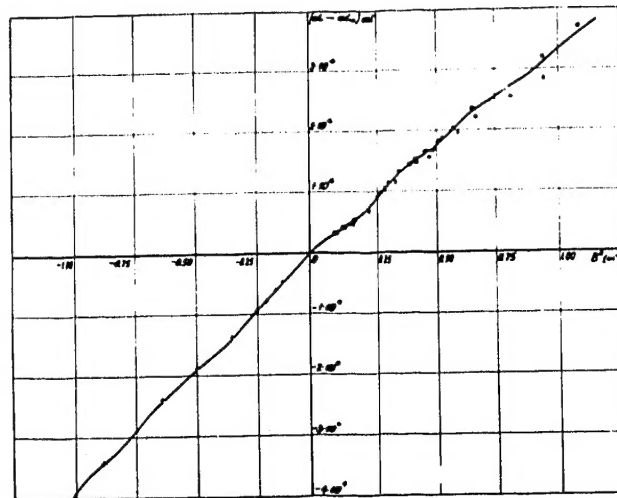


Fig.I4. The decay constant α as a function of B^2 for water.
 x- experiment [I7]; o- experiment [I5];
 •- experiment [I6].

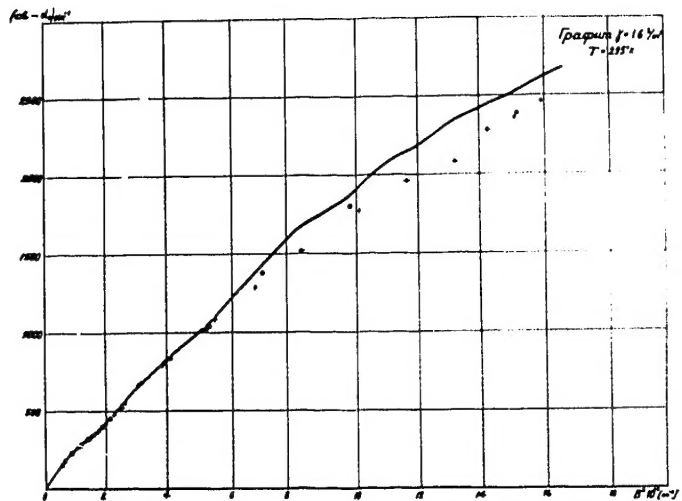


Fig.I5. The decay constant α as a function of B^2 for graphite
 x- experiment [I9] ; o- experiment [20].